JJMIE

Volume 8 Number 3, June. 2014
ISSN 1995-6665
Pages 143- 151

Jordan Journal of Mechanical and Industrial Engineering

Experimental Investigations on the Electrochemical Machining Characteristics of Monel 400 Alloys and Optimization of Process Parameters

[1*]M.Kalaimathi, [1]G.Venkatachalam and [2]M.Sivakumar

[1]*School of mechanical and building sciences,VIT University, Vellore-632014, TN, India*
[2]*Department of mechanical engineering,Sree Sowdambika College of engineering, Aruppukkottai-626134, TN, India*

Received 17 Dec 2013 *Accepted 16 Jun 2014*

Abstract

Monel 400 alloys are used in various fields such as aerospace industries, marine industries, etc. It is very difficult to machine Monel 400 alloys using conventional machine tools. The Electrochemical Machining (ECM), an advanced manufacturing process, is a natural choice for machining Monel 400 alloys. The present work is carried out to investigate the influence of ECM process parameters, such as applied voltage (V), inter electrode gap (IEG) and electrolyte concentration (EC), on material removal rate (MRR) and surface roughness (Ra) during machining Monel 400 alloys. An aqueous sodium chloride (NaCl) is used as a basic electrolyte in the electrochemical machining of Monel 400 alloys. The experimental strategy is based on a response surface methodology. The effects of process parameters as well as their interactions are investigated and the process parameters are optimized through the desirability function of the response surface methodology. The microstructure of the Monel 400 alloys specimen, machined with ECM, is studied to understand the effect of electrolyte and other parameters during the machining.

Keywords: *Electrochemical Machining (ECM), Material Removal Rate (MRR), Surface Roughness (Ra), Monel 400 Alloys, Response Surface Methodology (RSM), Desirability Function (DF).*

Nomenclature

V :Voltage between tool and work piece (V)
IEG :Inter electrode gap between tool and work piece (mm)
EC :Electrolyte concentration (grams per litre)
MRR :Material removal rate (grams per minute)
R_a : Surface roughness (μm)
RSM : Response surface methodology
CCD : Central composite design
DF : Desirability function

1. Introduction

Electrochemical machining (ECM) is a non-contact metal removing process, which is used to shape the work piece by anodic dissolution process. ECM has traditionally been used in with difficult-to-cut materials and with complex geometry. A D.C. voltage (5-30 V) is applied across the IEG between pre-shaped cathode tool and an anode work piece. The electrolyte flows at a high speed through the IEG. The current density is usually 20 to 200 A/cm^2. The anodic dissolution rate, which is governed by Faraday's laws of electrolysis, depends on the electrochemical properties of the metal, electrolyte properties and electric current/voltage supplied. ECM generates an approximate mirror image of the tool on the work piece [1]. The metal hydroxides and other by-products generated during the machining are removed from the gap by the high velocity of electrolyte flow. ECM process, a mechanical forceless machining with no thermally influenced machining zones, produces a high surface quality and low roughness. Tool design, pulsed current, micro-shaping and finishing, numerical control, environmental concerns and hybrid processes are very important in the utilization of the full potential of ECM [2]. The demand for the micro products and components of difficult-to–machine materials, such as tool steel, carbides, super alloys and titanium alloys, is rapidly increasing in automotive, aerospace, electronics, optics, medical devices and communication industries. These materials pose many challenges to conventional machining processes, such as turning and milling. Hence, it necessitates the machining of these materials with ECM. Advantages of ECM over other traditional machining processes include its applicability, regardless of material hardness, no tool wear, comparable high MRR, smooth and bright surface and the production of components of complex geometry with stress-free and crack-free surfaces [3]. ECM has been

* Corresponding author. e-mail: mkm1979@rediffmail.com

applied in many industrial applications including turbine blades, engine castings, bearing cages, gears, dies and moulds and surgical implants. ECM is also more suitable for large scale production.

Monel 400 alloy is an excellent alloy among all the commonly used nickel based alloys for its corrosion resistance and toughness. It is primarily used in industries such as nuclear, aerospace, missile, and marine. Monel alloys work hardens rapidly as it undergoes high strains during machining. This hardening effect slows further machining. Therefore, it is very difficult to machine these alloys using conventional machine tools. Tool failure is the common result in the machining of Monel 400 alloys with conventional methods due to the work hardening effect. ECM could therefore be a cost-effective alternative for Monel 400 alloys and could become more and more significant in the near future. Several works have been reported in the literature for machining of nickel based alloys using different non-conventional machining methods. The improvement in the machinability of nickel base and titanium alloys with ceramic tools was extensively analysed by Ezugwu *et al.* [4, 5]. Liu *et al.* studied the characterization of nickel alloy micro-holes using micro-EDM together with grinding [6]. Ulutan *et al.* analyzed machining induced surface integrity for titanium alloys and nickel-based alloys. Problems with residual stresses, white layer and work hardening layers, as well as micro-structural alterations were studied to improve surface qualities of end products [7]. Selvakumar *et al.* [8, 9] investigated the machining suitability of Monel 400 alloys with wire-cut electrical discharge machining (WEDM). Die corner accuracy and surface roughness of Monel 400 alloys were considered as responses; Selvakumar *et al.* [8, 9] also studied various WEDM process parameters' influence.

Significant attempts [10-13] have been made on machining of nickel based alloys. But all these machining methods, reported in the literature, result in the reduction of tool life including WEDM. But the machining suitability of Monel 400 alloys, with ECM process, is not widely reported in the literature. Hence, in the present work, ECM has been used to study the machining characteristics of Monel 400 alloys. The aim of this work is to develop the comprehensive mathematical models for correlating the interactive and higher-order influences of the various machining parameters such as applied voltage (V), inter electrode gap (IEG) and electrolyte concentration (EC) on the prime machining performances, i.e., material removal rate (MRR) and surface roughness (R_a) for the effective utilization of the full potential of ECM. Response surface methodology (RSM) is employed to plan and analyze the experiments. The objective of using the RSM is not only to investigate the response over the entire factor space, but also to locate the region of the interest where the response reaches its optimum or near optimum value. By carefully studying the response surface model, the combination of the factors which gives the best response, can then be established [14]. RSM was implemented as an effective experimental strategy in end milling by Kadirgama *et al.* [15].

2. Experimentation

Schematic diagram of ECM set-up is shown in Figure 1. The process parameters, selected for the present investigation, are EC, V and IEG because of the significant influence on the ECM performances [16-19]. Their effects on the MRR and R_a are tested through the set of the planned experiments based on central composite design (CCD) of RSM. Table.1 shows the factors and their levels in coded and actual values. The levels of each factor were chosen as -2, -1, 0, 1, 2 in closed form to have a rotatable design. The coded values were obtained from the following equation:

$$X_i = \frac{Chosen\ parametric\ values - Central\ rank\ of\ parameters}{Interval\ of\ variation} \quad (1)$$

Where, X_i is the coded values of the variables IEG, V and EC, respectively.

The design requires 20 experiments for the three variables. The design was generated and analysed using DESIGN EXPERT statistical package.

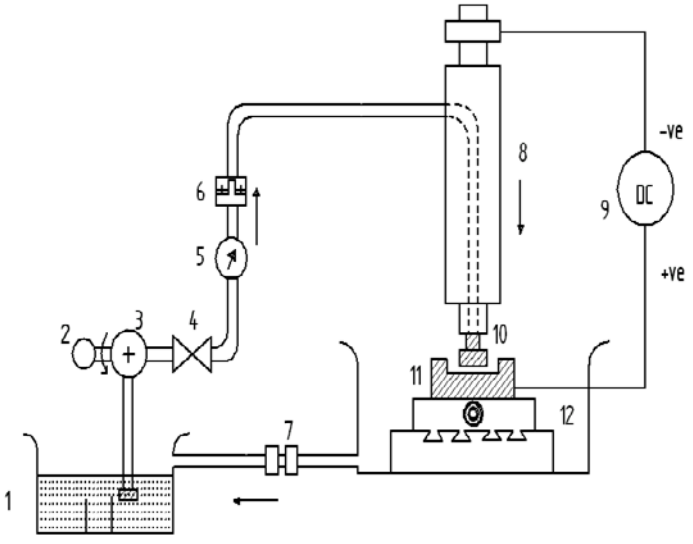

Figure 1. Schematic diagram of ECM

1. Electrolyte tank,
2. Motor,
3. Pump,
4. Flow control,
5. Pressure gauge,
6. Flow meter,
7. Filter
8. Tool feed mechanism,
9. Low voltage high current DC supply,
10. Tool,
11. Work piece (Monel 400alloy),
12. Workholding vice Tool holder.

Figure 2 shows a photographic view of the experimental apparatus of the ECM. Figure 3(a) and Figure 3(b) represent the 3D model and the cross sectional view of the tool used in this work. Commercially obtained Monel 400 alloys were used as a test specimen. The chemical composition (weight %) of Monel 400 alloys is as follows: C: 0.047, Si: 0.172, Mn: 1.03, P: 0.012, S: 0.01, Cr: 0.1, Mo: 0.1, Fe: 1.66, V: 0.029, W: 0.1, Cu: 29.24, Al: 0.01, Co: 0.103, Nb: 0.1, Ti: 0.047, Mg: 0.031, and Ni: 67.4.

Table 1. Process Parameters and their values at different levels

Symbol	Process parameters	Levels				
		-2	-1	0	1	2
X_1	Inter electrode gap, IEG (mm)	0.1	0.2	0.3	0.4	0.5
X_2	Voltage, (V)	10	15	20	25	30
X_3	Electrolyte concentration, EC (grams per litre)	100	130	160	190	220

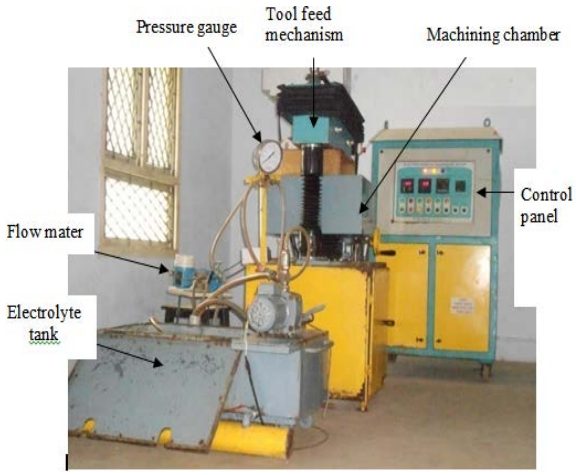

Figure 2. Electrochemical machining set-up

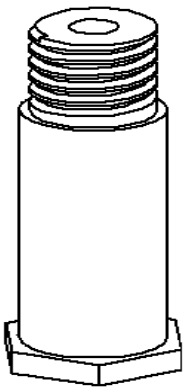

Figure 3. (a) 3D model of tool

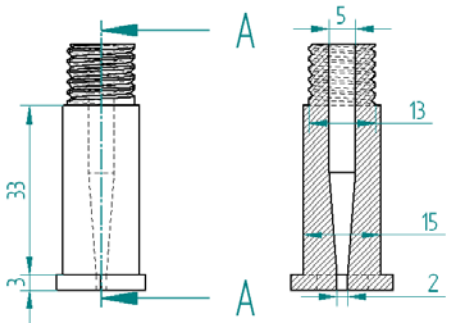

Figure 3. (b) Cross sectional view of tool

The MRR and R_a were observed for a various set of experiments with a different combination of process parameters based on RSM. Using RSM, a comprehensive mathematical model is developed for correlating the interactive and higher-order influences of various machining parameters on the dominant machining criteria, i.e., the MRR and the surface roughness (R_a). The general second order polynomial response surface mathematical model, which analyses the parametric influences on the various response criteria, is given below:

$$Y_u = b_o + \sum_{i=1}^{n} b_i X_{iu} + \sum_{i=1}^{n} b_{ii} X^2_{iu} + \sum_{j>i}^{n} b_{ij} X_{iu} X_{ju} + e_u \quad (2)$$

Where Y_u represents the corresponding response, i.e., MRR and R_a of the ECM process in the present work. The value n indicates the number of machining parameters. The terms b_i, b_{ii}, b_{ij} are the second order regression coefficients. The second term under the summation sign of this polynomial equation attributes to the linear effects and the fourth term of the equation represents the interactive effects of the parameters. The collection of experimental data adopts the CCD in order to fit the quadratic model of y_u. The experiment has been carried out according to the designed experiment based on CCD which is illustrated in Table 2.

In this work, MRR was measured based on weight loss during machining time:

$$MRR = \frac{LW}{MT} \text{ grams per minute} \quad (3)$$

Where, LW-Loss of weight, i.e., weight difference of work piece before and after machining in grams MT-Machining time in minutes.

Weights were measured using Sartorius (BS 423S) balance with an accuracy of 0.001g. The surface roughness (R_a) value is the indicator of the technical surface quality of an engineering product. In this work, R_a was measured using the Mitutoyo (SJ-201) surface roughness tester with a sampling length of 10 mm. Roughness measurements, in the transverse direction, on the work pieces were repeated three times and the average of the three measurements of surface roughness(R_a) values was recorded.

Table 2. Experimental observation

Exp. No.	Inter electrode gap (IEG)		Voltage (V)		Electrolyte concentration (EC)		MRR (grams/minute)	R_a (μm)
	Coded X_1	Actual (mm)	Coded X_2	Actual (V)	Coded X_3	Actual (grams/litre)		
1	-1	0.2	1	25	-1	130	0.577	2.02
2	0	0.3	0	20	0	160	0.458	1.79
3	1	0.4	-1	15	-1	130	0.395	2.78
4	0	0.3	0	20	0	160	0.495	1.97
5	1	0.4	1	25	1	190	0.617	2.82
6	-1	0.2	-1	15	1	190	0.294	1.23
7	0	0.3	0	20	0	160	0.494	2.13
8	0	0.3	0	20	2	220	0.381	1.27
9	-2	0.1	0	20	0	160	0.563	1.27
10	0	0.3	0	20	-2	100	0.527	2.37
11	0	0.3	2	30	0	160	0.620	3.50
12	0	0.3	-2	10	0	160	0.417	2.19
13	2	0.5	0	20	0	160	0.504	2.45
14	0	0.3	0	20	0	160	0.451	1.82
15	0	0.3	0	20	0	160	0.518	1.91
16	0	0.3	0	20	0	160	0.518	1.82
17	1	0.4	-1	15	1	190	0.322	2.05
18	-1	0.2	1	25	1	190	0.585	2.22
19	-1	0.2	-1	15	-1	130	0.492	1.35
20	1	0.4	1	25	-1	130	0.402	2.76

3. ANOVA Analysis

The analysis of variance is performed for the model adequacy checking, which includes a test for the significance of the regression model, model coefficients and lack of fit. ANOVA is mainly carried out to analyse the variation among the groups. This is done by *F-test* at 95% confidence level. Significance and insignificance are determined by comparing the F-values with standard tabulated values at the corresponding degrees of freedom and 95% confidence level. The values of "Prob > F" less than 0.05 indicates that the model and its terms are significant. The values which are greater than 0.1 indicate that the model terms are not significant[14].

3.1. Material Removal Rate (MRR)

The quadratic model is statistically significant for the analysis of MRR. The details of ANOVA for the response surface quadratic model along with the partial sum of squares on MRR are given in the Table 3.

The F-value of the source “Model” 7.91 implies that the model is significant. This means that the regression model provides an excellent explanation of the relationship between the factors and the MRR. In this case, V, IEG*EC, V*EC are significant model terms. The lack of fit “F-value” 3.84 is less than the tabulated value, which means that the developed model is adequate.

Table 3. ANOVA for response surface quadratic model of MRR

Source	Sum of Squares	DF	Mean Square	F Value	Prob > F	Significance
Model	0.140 00	9	0.016 00	7.91	0.001 7	significant
IEG	0.006 84	1	0.006 84	3.41	0.094 6	
V	0.077 00	1	0.077 00	38.18	0.000 1	
EC	0.007 31	1	0.007 31	3.64	0.085 4	
IEG^2	0.001 43	1	0.001 43	0.71	0.418 3	
V^2	0.000 62	1	0.000 62	0.31	0.589 6	
EC^2	0.003 80	1	0.003 80	1.90	0.198 5	
IEG*V	0.000 70	1	0.000 70	0.35	0.567 4	
IEG*EC	0.014 00	1	0.014 00	6.91	0.025 2	
V*EC	0.030 00	1	0.030 00	15.00	0.003 1	
Residual	0.020 00	10	0.002 01			
Lack of Fit	0.016 00	5	0.003 18	3.84*	0.083 1	not significant
Pure Error	0.004 15	5	0.000 83			
Total	0.160 00	19				

F0.05(5,5)=5.05,*Not significant

Table 4. ANOVA for response surface quadratic model of surface roughness(R_a)

Source	Sum of Squares	DF	Mean Squares	F Value	Prob>F	Significance
Model	6.220 00	9	0.690 00	18.13	< 0.000 1	Significant
IEG	2.220 00	1	2.220 00	58.14	< 0.000 1	
V	1.580 00	1	1.580 00	41.50	< 0.000 1	
EC	0.490 00	1	0.490 00	12.80	0.005 0	
IEG^2	0.001 35	1	0.001 35	0.035	0.854 7	
V^2	1.430 00	1	1.430 00	37.43	0.000 1	
EC^2	0.007 54	1	0.007 54	0.20	0.666 1	
IEG*V	0.100 00	1	0.100 00	2.71	0.130 9	
IEG*EC	0.069 00	1	0.069 00	1.81	0.208 3	
V*EC	0.150 00	1	0.150 00	3.99	0.073 8	
Residual	0.380 00	10	0.038 00			
Lack of Fit	0.300 00	5	0.059 00	3.54*	0.095 7	not significant
Pure Error	0.084 00	5	0.017 00			
Cor Total	6.600 00	19				

$F_{0.05}(5,5)=5.05$,*Not significant

The suitable regression model for the response MRR is given below:

$$MRR = 2.2427 - 2.0515 * IEG - 0.04595 * V - 0.01305 * EC + 0.01387 * IEG * EC + 0.00041 * V * EC \quad (4)$$

(Coefficient of determination R^2=0.70)

3.2. Surface Roughness(Ra)

The quadratic model is statistically significant for the analysis of surface roughness. The details of ANOVA for the response surface quadratic model along with the partial sum of squares on surface roughness are given in the Table 4:

The model F-value of 18.13 implies the model is significant. In this case, IEG, V, EC, V^2 are significant model terms. The "Lack of Fit F-value" of 3.54 implies there is a 9.57% chance that a "Lack of Fit F-value" which is due to noise.

The second order polynomial equation for R_a is fit as shown below:

$$R_a = 3.8174 + 13.661 * IEG - 0.3973 * V - 0.00876 * EC + 0.00953 * V^2 - 0.22725 * IEG * V - 0.03096 * IEG * EC + 0.001 * V * EC \quad (5)$$

This model can be used to navigate the design space.

4. Results and Discussion

4.1. Parametric Influence on MRR

Based on the mathematical model (Eq. 4) which is developed through the CCD of the response surface methodology, the effect of the various process parameters' influence on the MRR has been analyzed. The contour plots were drawn for various combinations of influencing parameters. The changes in the intensity of the shade in the plot represent the change in the MRR. Figures 4(a) – 4(c) represent the influence of parameters such as EC, V and IEG on MRR. Figure 4(a) exhibits the influence of the applied voltage and IEG on MRR. The increase in the voltage increases the machining current in the inter electrode gap (IEG), thereby increasing the MRR.

Smaller IEG increases the rapid anodic dissolution as a result of higher current density [15]. This conforms to the fundamental machining mechanism of ECM. Figure 4(b) represents the effect of IEG and EC on the MRR. The mobility of ions in the high concentration of electrolyte in the small IEG is disturbed. Therefore, it results in poor MRR. But, the smaller IEG and the moderate concentration allow more ions for ionisation, which results in increasing the MRR. This can be seen from the Figure 4(b).

Figures 5-7 highlights the effect of voltage with EC 160 grams per liter and IEG 0.3 mm on surface roughness (Ra) and MRR. Figure 5 clearly exhibits the very good anodic dissolution at high voltage (30 V). Higher voltages break the surface film and its disruption is non-uniform that results deep grain boundary attack of the metal surface. At low voltage (10 V), dissolution is poor, which could be seen in Figure 6.

High and uniform dissolution occurs at 20 V as observed in Figure 7. This voltage is sufficient to make a uniform dissolution. It can be observed that the increase in electrolyte concentration (EC) increases MRR. The increase in both voltage (V) and EC enhances the MRR considerably which is attributed to the effect of the increase in the conductance of electrolyte. This can be seen in Figure 4(c).

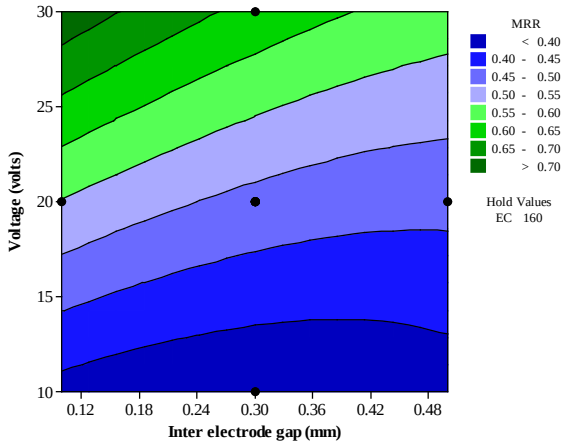

(a)Influence of V and IEG on MRR

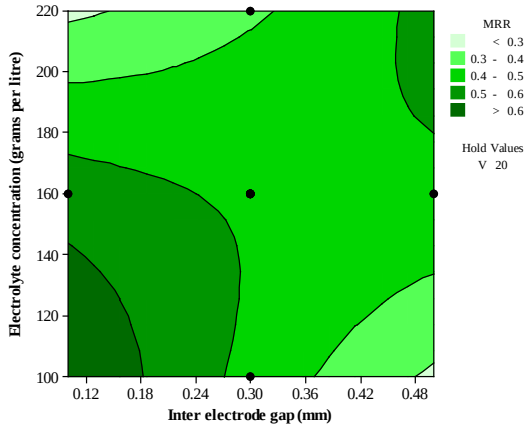

(b) Influence of EC and IEG on MRR

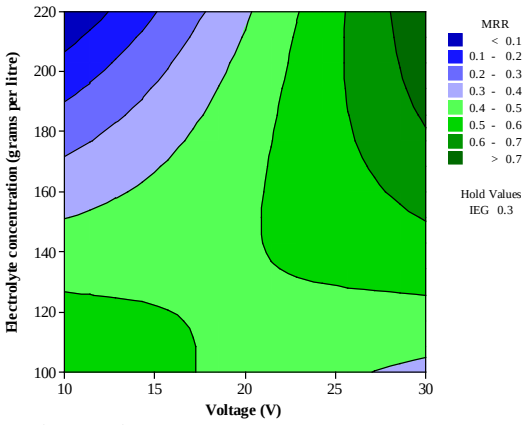

(c)Influence of EC and V on MRR

Figure 4. Contour Plots of MRR

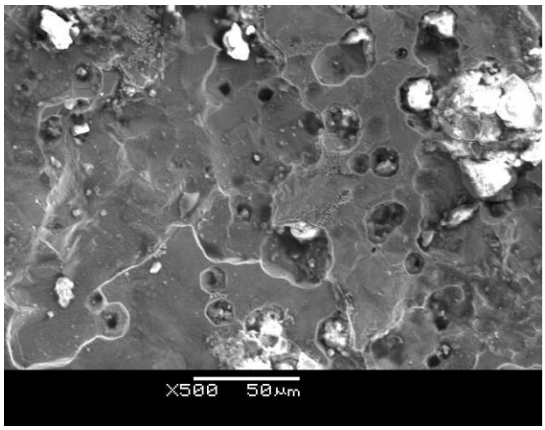

Figure 5. High and non uniform dissolution at 30 V

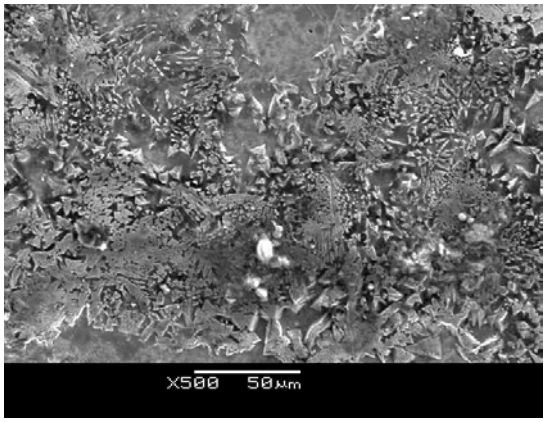

Figure 6. Moderate dissolution at 10 V

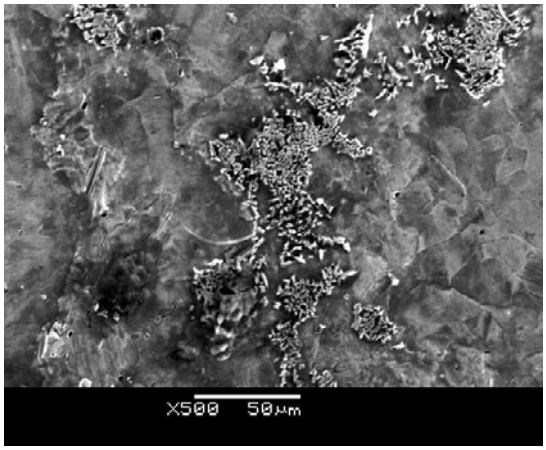

Figure 7. High and uniform dissolution at 20 V

4.2. Parametric Influence on Ra

Figures 9(a) -9(c) illustrate the influence of parameters on the surface roughness (R_a) in aqueous NaCl environment. Figure 9(a) demonstrates the effect of the applied voltage (V) and IEG on the surface roughness (R_a) of machined Monel 400 alloys. Higher voltage enhances the anodic dissolution drastically but with some excessive heating, which leads to a poor surface finish. Low voltage is sufficient to get a good surface finish. But higher IEG reduces the current density in the gap which leads to non-uniform metal removal and results in a poor surface finish as shown in Figure 8.

Higher electrolyte concentration and voltage lead to a rapid metal dissolution which results in a higher R_a. A slightly high electrolyte concentration with a low IEG produces low R_a. This is due to the higher current density in the smaller IEG with a uniform metal dissolution because of an adequate concentration.

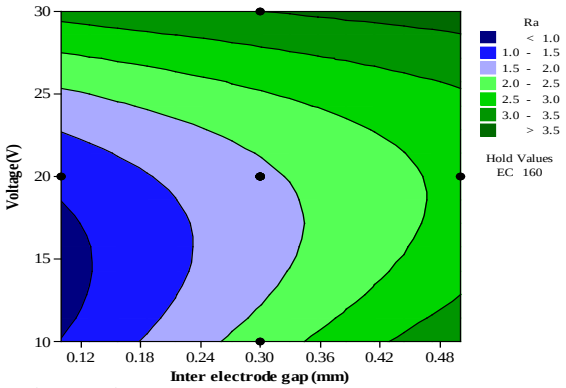

a)Influence of V and IEG on R_a

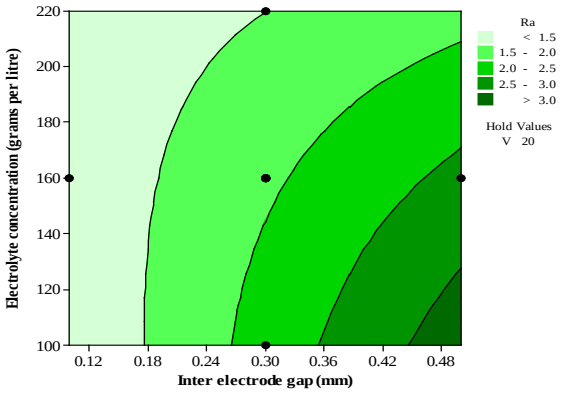

b)Influence of EC and IEG on R_a

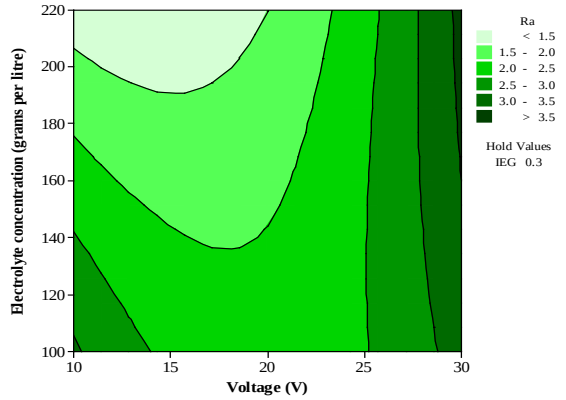

c)Influence of EC and V on R_a

Figure 9. Contour plots of surface roughness(R_a)

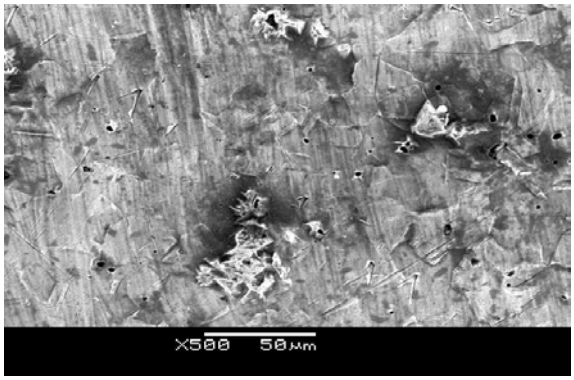

Figure 8. Poor dissolution at high IEG 0.5 mm

5. Response Surface Optimization

In RSM, multiple responses are optimized with the steepest ascent/descent method by the desirability function (DF). DF is one of the most extensively used methods for multi-response optimization. It transforms each response y_i into an individual desirability function $d_i(y_i)$ that varies in the range (0, 1). It increases as the corresponding response value becomes more desirable. Depending upon the nature of the responses (y_i), the desirability functions $d_i(y_i)$ will be maximized/minimized, or assigned to a target value. The individual desirability $d_i(y_i)$ will be as follows:

$$d_i(y_i) = 0 \ \ if \ \ y_i(x) \leq L_i \quad (6)$$

$$d_i(y_i) = \left(\frac{y_i(x)-L_i}{T_i-L_i}\right)^r \ \ if \ \ L_i \leq y_i(x) \leq T_i \quad (7)$$

$$d_i(y_i) = \left(\frac{y_i(x)-U_i}{T_i-U_i}\right)^r \ \ if \ \ T_i \leq y_i(x) \leq U_i \quad (8)$$

$$d_i(y_i) = 0 \ \ if \ \ y_i(x) > U_i \quad (9)$$

Where, $\boldsymbol{x}$ is the parameters, i.e., IEG, V, EC
L_i and U_i are lower and upper acceptable bounds of y_i ,
T_i *is* target values desired for i^{th} response, where $L_i < T_i < U_i$
r is the parameter that determines the shape of $d_i(y_i)$.

The individual desirability functions are then combined using the geometric mean, which gives the *Composite desirability D*:

$$D = ((d_1(y_1) * d_2(y_2) * \ldots . * d_m(y_m))^{\frac{1}{m}} \quad (10)$$

Table 5. Constraints

Variables		Goal	Lower bound (L_i)	Upper bound (U_i)
x_i	IEG	In the range	0.2	0.4
	V	In the range	15	25
	EC	In the range	130	190
y_u	MRR	Maximize	0.294	0.6298
	R_a	Minimize	1.23	3.5

The best composite desirability (0.822) is established at the following machining conditions.

IEG=0.2mm,V=18 V, EC=130 grams per litre, MRR=0.5546 grams per minute, Ra=1.5216 µm

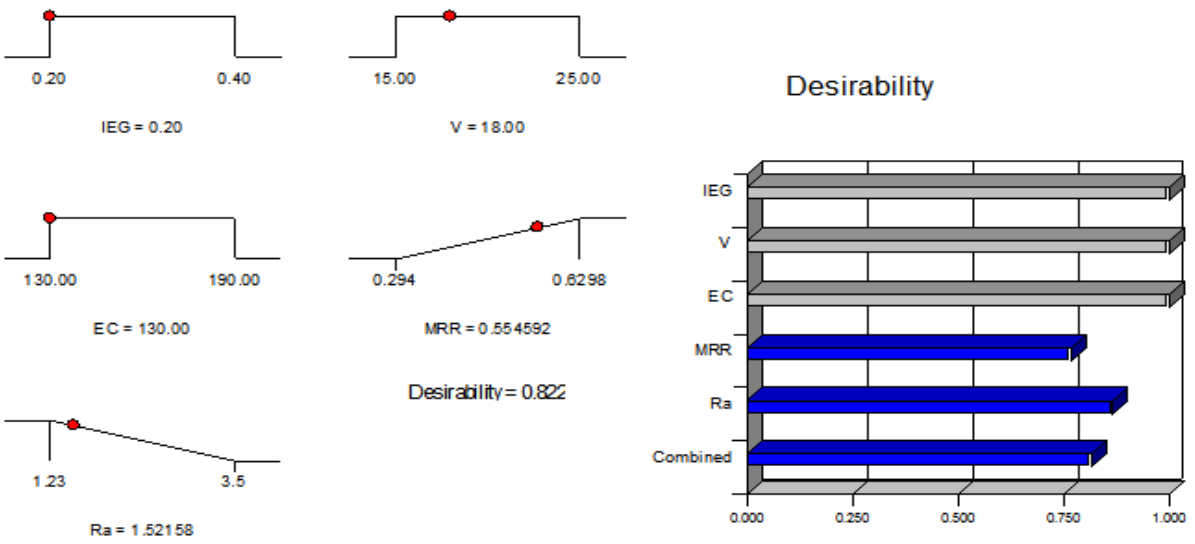

Figure 10. Ramps and bar chart

Figure 10 represents the ramps and bar chart at the optimal machining conditions.

6. Conclusion

An attempt has been made in this work to highlight the influence of ECM process parameters on the machining performances, i.e., MRR, R_a for Monel 400 alloys. Response surface methodology was employed to analyze the ECM process. Mathematical models have also been developed based on the RSM approach for correlating the MRR and R_a with process parameters. The adequacy of the developed mathematical model has been tested through the analysis of variance (ANOVA). The results of the analysis justify the closeness of the fit of the mathematical model at 95% confidence level. The influence of different process parameters on machining performance criteria are exhibited though contour plots. It is clear from the response contour plot of MRR that both the MRR and surface roughness increase with the increase in the voltage. The increase in the voltage causes the excessive heating of electrolyte and a corresponding deterioration of the work piece surface which increases the surface roughness. Electrolyte concentration of 160 grams per liter and IEG 0.3 mm provide good MRR and R_a. From the developed mathematical model, the optimal machining parametric combination, i.e., IEG=0.2 mm,V=18 V and EC=130 grams per liter was found out to achieve the maximum material removal rate, i.e., 0.5546 grams per minute and minimum surface roughness as 1.5216 µm. The effective utilization of ECM for Monel 400 alloys for achieving the best material removal rate (MRR) and surface roughness (R_a) has been attempted in this work.

References

[1] Rajurkar K.P, Sundaram M.M and Malshe A. P, "Review of Electrochemical and Electro discharge Machining", Procedia CIRP,Vol. 6 (2013) 13-26, The Seventeenth CIRP Conference on Electro Physical and Chemical Machining (ISEM).

[2] Rajurkar K.P, Zhu D, McGeough J.A, Kozak J and De Silva A, "New Developments in Electro-Chemical Machining", CIRP Annals - Manufacturing Technology, Vol. 48 (1999) Issue 2, 567–579.

[3] Sundaram M.M. and Rajurkar K.P, "Electrical and Electrochemical Processes, in Intelligent Energy Field Manufacturing", CRC Press (2010) 173-212.

[4] Ezugwu E.O, "Key improvements in the machining of difficult-to-cut aerospace super alloys', International Journal of Machine Tools and Manufacture, Vol. 45(2005) Issues 12–13, 1353–1367

[5] Ezugwu E.O, Bonney J, Fadare D.A and Sales W.F, "Machining of nickel-base, Inconel 718, alloy with ceramic tools under finishing conditions with various coolant supply pressures", Journal of Materials Processing Technology, Vol. 162–163(2005) issue 15, 609–614.

[6] Liu H.S, Yan B.H , Huang F.Y and Qiu K.H, "A study on the characterization of high nickel alloy micro-holes using micro-EDM and their applications", Journal of Materials Processing Technology, Vol. 169(2005) Issue 3, 418–426.

[7] Durul Ulutan and Tugrul Ozel, "Machining induced surface integrity in titanium and nickel alloys: A review", International Journal of Machine Tools and Manufacture, Vol. 51(2011) Issue 3, 250–280.

[8] Selvakumar G, Sarkar K and Mitra S, "Experimental analysis on WEDM of Monel 400 alloys in a range of thickness", International Journal of Modern Manufacturing Technologies, Vol. IV (2012) 113-120.

[9] Selvakumar G,Sarkar K and Mitra S, "Experimental investigation on die corner accuracy for wire electrical discharge machining of Monel 400 alloy", Proc IMechE Part B:J Engineering Manufacture, Vol. 226 (2012) 10, 1694–1704.

[10] Theisen W and Schuermann A, "Electro discharge machining of nickel–titanium shape memory alloys", Materials Science and Engineering: A, Vol. 378 (2004) Issues 1–2, 200–204.

[11] Kaynak Y, Karaca H.E, Noebe R.D and Jawahir I.S, "Tool-wear analysis in cryogenic machining of *NiTi* shape memory alloys: A comparison of tool-wear performance with dry and MQL machining Wear", Vol. 306 (2013) Issues 1–2, 51–63.

[12] Curtis D.T, Soo S.L, Aspinwall D.K and Sage C, "Electrochemical super abrasive machining of a nickel-based aero engine alloy using mounted grinding points", CIRP Annals - Manufacturing Technology", Vol. 58 (2009) Issue 1,173–176.

[13] Gao D, Hao Z, Han R, Chang Y and Muguthu J.N, "Study of cutting deformation in machining nickel-based alloy Inconel 718", International Journal of Machine Tools and Manufacture, Vol. 51(2011) Issue 6, 520–527.

[14] Montgomary Doughlas C, "Design and Analysis of Experiments" 5th edition (1997), John wiley publications,Singapore.

[15] Kadirgama K, Noor M.M, Zuki N.M, Rahman M.M, Rejab M.R.M, Daud R and Abou-El-Hossein K. A, "Optimization of Surface Roughness in End Milling on Mould Aluminium Alloys (AA6061-T6) Using Response Surface Method and Radian Basis Function Network", Jordan Journal of Mechanical and Industrial Engineering, Vol. 2 (2008) No.4, 209-214.

[16] Senthilkumar C, Ganesan G and Karthikeyan R, "Study of electrochemical machining characteristics of Al/SiC_p Composites", International Journal of Advanced Manufacturing Technology 43 (2009) 256-263.

[17] Rama Rao S and Padmanabhan G,"Effect of process variables on metal removal rate in electrochemical machining of Al-B4C composites", Archives of Applied Science Research, Vol. 4 (2012) 4, 1844-1849.

[18] Rama Rao S and Padmanabhan G, "Linear Modelling of the Electrochemical Machining Process Using Full Factorial Design of Experiments", Journal of Advanced Mechanical Engineering, Vol. 1 (2013) 13-23.

[19] Senthil Kumar K.L, Sivasubramanian R and Kalaiselvan K, "Selection of Optimum Parameters in Non-Conventional Machining of Metal Matrix Composite", Portugaliae Electrochimica Acta, Vol. 27 (2009) 4, 477-486.